Thermochimica Acta 517 (2011) 74–80

Contents lists available at ScienceDirect

Thermochimica Acta

journal homepage: www.elsevier.com/locate/tca

Crystallization kinetics and morphology studies of biodegradable poly(ethylene succinate)/multi-walled carbon nanotubes nanocomposites

Siyu Zhu, Yuanyuan Zhao, Zhaobin Qiu*

State Key Laboratory of Chemical Resource Engineering, Key Laboratory of Carbon Fiber and Functional Polymers, Ministry of Education, Beijing University of Chemical Technology, Beijing 100029, China

ARTICLE INFO

Article history:
Received 16 November 2010
Received in revised form 14 January 2011
Accepted 23 January 2011
Available online 2 February 2011

Keywords:
Crystallization
Biodegradable polymer
Poly(ethylene succinate)
Multi-walled carbon nanotubes
Nanocomposite

ABSTRACT

Biodegradable poly(ethylene succinate) (PES)/carboxyl-functionalized multi-walled carbon nanotubes (f-MWNTs) nanocomposites were prepared through solution casting method. Scanning electron microscopy observations show a homogeneous dispersion of f-MWNTs throughout the PES matrix. Effect of f-MWNTs on the crystallization behavior of PES was investigated in detail under different crystallization conditions in this work. For both nonisothermal and isothermal melt crystallization, the addition of f-MWNTs enhances the crystallization of PES apparently due to the heterogeneous nucleation effect. The Ozawa method does a good of describing the nonisothermal melt crystallization of neat PES and its nanocomposites. The Avrami method does a good of describing the isothermal melt crystallization kinetics of neat PES and its nanocomposites; moreover, the overall crystallization rate of PES is enhanced significantly while the crystallization mechanism remains unchanged in the presence of f-MWNTs in the nanocomposites. The crystal structure of PES remains unchanged in the PES/f-MWNTs nanocomposites despite the presence of f-MWNTs.

1. Introduction

Biodegradable aliphatic polyesters have attracted a great deal of attention due to their potential applications in the fields related to environmental protection and resource recycles in the last two decades. Poly(ethylene succinate) (PES) is one of the biodegradable synthetic polyesters. The chemical structure is $(-OCH_2CH_2O_2CCH_2CH_2CO-)_n$. The crystal structure, biodegradability, crystallization kinetics, and melting behavior of PES have been studied in detail [1–7]. In many crystalline/amorphous polymer blends and crystalline/crystalline polymer blends, PES is often used as an essential component. Through modifying the crystallization and morphology of PES in the polymer blends, the overall properties of PES may be improved significantly. Miscibility, crystallization kinetics, semicrystalline morphology, and mechanical properties of miscible crystalline/crystalline polymer blends with PES being one component have been investigated extensively. For example, poly(ethylene oxide) (PEO)/PES and poly(hydroxybutyrate) (PHB)/PES blends are just two typical miscible crystalline/crystalline polymer blends [8–14].

Carbon nanotubes (CNTs) were first reported by Iijima [15]. CNTs consist of concentric cylinders of graphite layers, and can be classified into two basic types, i.e., single-walled carbon nanotubes (SWNTs) and multi-walled carbon nanotubes (MWNTs). They possess high flexibility and low mass density, and the large aspect ratio of the CNTs imparts a significant increase in the modulus of the composites. Because of their excellent mechanical, electrical and thermal properties, CNTs have been considered as ideal reinforcing fillers in the fabrication of polymer nanocomposites [16–20]. Consequently, combining biodegradable polymers with a small quantity of CNTs must be of great interest and use from both academic and industrial perspectives. Some biodegradable polymer/CNTs nanocomposites have been reported in the literatures [21–29].

However, to our knowledge, PES/multi-walled carbon nanotubes nanocomposites have not been reported yet until now. In the present work, PES/MWNTs nanocomposites were prepared via solution casting method using chloroform as a mutual solvent; moreover, the crystallization and morphology of PES/MWNTs nanocomposites at different MWNTs loadings were studied with various techniques in detail in this work. It is expected that the results reported herein will be of interest and importance for a better understanding of the relationship between structure and properties of biodegradable polymer nanocomposites.

2. Experimental details

2.1. Materials and preparation of PES/f-MWNTs nanocomposites

PES was purchased from Sigma–Aldrich (Shanghai) Trading Co. Ltd. The carboxyl-functionalized multi-walled carbon nanotubes

* Corresponding author. Tel.: +86 10 64413161; fax: +86 10 64413161.
E-mail addresses: zbqiu99@yahoo.com, qiuzb@mail.buct.edu.cn (Z. Qiu).

0040-6031/$ – see front matter © 2011 Elsevier B.V. All rights reserved.
doi:10.1016/j.tca.2011.01.031

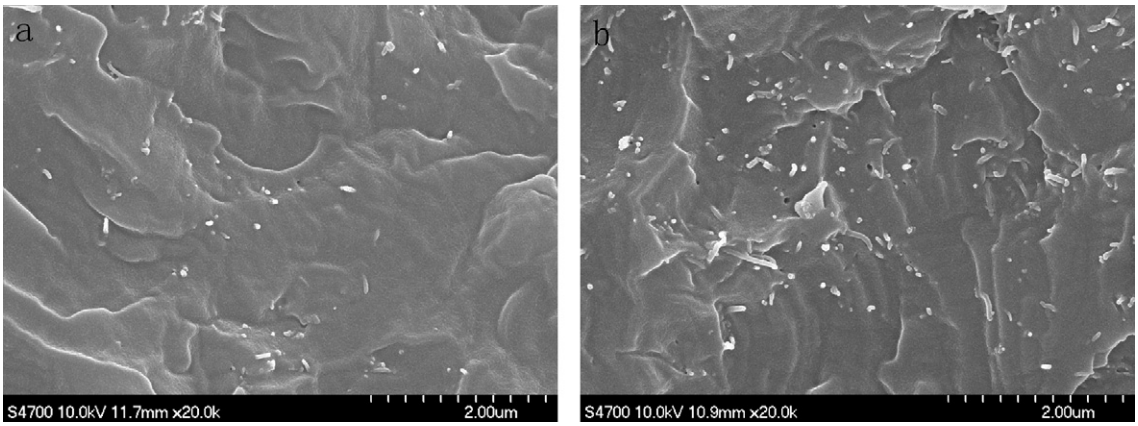

Fig. 1. SEM images of fracture surface for (a) 99.5/0.5 and (b) 98/2.

(f-MWNTs) were purchased from Chengdu Institute of Organic Chemistry, Chinese Academy of Sciences. The outer diameter is around 30–50 nm, and the –COOH content on the surface of MWNTs is about 0.73 wt% according to the supplier.

The PES/f-MWNTs nanocomposites were prepared through a solution casting method. For the fabrication of nanocomposites, PES was mixed with the addition of various f-MWNTs contents, specified as 0.5, 1, and 2 wt% in the polymer matrix, respectively. Chloroform was used as the mutual solvent. The appropriate amount of f-MWNTs was added into chloroform and then was sonicated with a KQ 3200E ultrasonic generator to make a uniformly dispersed suspension. PES was placed into chloroform and stirred for 1 h to dissolve PES completely. Next, the PES solution was added to the f-MWNTs suspension. The PES/f-MWNTs solution was further stirred for 3 h and then poured into a dish to evaporate the solvent at 40 °C in air. The sample was further dried at 60 °C under vacuum for 3 days to remove the solvent completely. In this work, neat PES and its three PES/f-MWNTs nanocomposites were abbreviated as 100/0, 99.5/0.5, 99/1, and 98/2, respectively, with the first number referring to PES while the second number referring to f-MWNTs.

2.2. Characterizations

A field emission scanning electron microscopy (S-4700, Hitachi Co., Japan) was used to observe morphology of the surfaces of PES/f-MWNTs nanocomposites fractured in liquid nitrogen. All the samples were coated with gold before examination.

Thermal analysis was carried out using a TA Instrument differential scanning calorimetry (DSC) Q100 with a Universal Analysis 2000. All operations were performed under nitrogen purge, and the weight of the samples varied between 4 and 5 mg. Two different procedures, i.e., nonisothermal melt crystallization and isothermal melt crystallization, were employed to study the crystallization behavior of neat PES and its nanocomposites. In the case of nonisothermal melt crystallization, the samples were first heated to 130 °C at 40 °C/min, held at 130 °C for 5 min to erase any thermal history, and then cooled to −30 °C at different constant cooling rates ranging from 1 to 5 °C/min. The crystallization peak temperature (T_p) was obtained from the cooling traces. In the case of isothermal melt crystallization, the samples were annealed at 130 °C for 5 min to erase any thermal history, cooled to the desired crystallization temperature (T_c) at 40 °C/min, and then maintained at T_c until the crystallization was complete. The exothermal traces were recorded for the later data analysis.

Spherulitic morphology of neat PES and the PES/f-MWNTs nanocomposites was observed under crossed polarizers by a polarizing optical microscopy (POM) (Olympus BX51) with a temperature controller (Linkam THMS 600). The samples were first annealed at 130 °C for 5 min to erase any thermal history and then cooled to 60 °C at 40 °C/min.

Wide angle X-ray diffraction (WAXD) patterns were recorded using a Rigaku D/Max 2500 VB2t/PC X-ray diffractometer from 10° to 30° at 3°/min. The Cu K_α radiation ($\lambda = 0.15418$ nm) source was operated at 40 kV and 200 mA. The samples were first pressed into films with a thickness of around 0.5 mm on a hot stage at 130 °C and then transferred into a vacuum oven at 64 °C for 24 h.

3. Results and discussion

3.1. Morphology and dispersion of f-MWNTs in the PES matrix

The surface of PES/f-MWNTs nanocomposites fractured in liquid nitrogen was observed with SEM to examine the distribution of f-MWNTs in the PES matrix. Parts a and b of Fig. 1 show the fracture surfaces of 99/0.5 and 98/2, respectively. The bright dots and lines are the ends of the broken f-MWNTs. Since some nanotubes seem to be pulled out of the section surface, the ends of individual f-MWNTs embedded in the matrix can be observed clearly. It can be seen from Fig. 1a that a fine dispersion of f-MWNTs is achieved, and there is no obvious aggregation of f-MWNTs throughout the PES matrix. Moreover, with increasing the f-MWNTs content up to 2 wt%, the homogeneous dispersion of f-MWNTs can still be observed as shown in Fig. 1b, indicating that the variation of f-MWNTs content from 0.5 to 2.0 wt% does not influence the dispersion and distribution of f-MWNTs in the polymer matrix significantly.

3.2. Effect of f-MWNTs on the nonisothermal melt crystallization of PES in the PES/f-MWNTs nanocomposites

As introduced in Section 2, nonisothermal melt crystallization of neat PES and its nanocomposites with different f-MWNTs loadings was first studied with DSC at various cooling rates ranging from 1 to 5 °C/min in this work. Fig. 2a shows the DSC cooling curves of neat PES and its nanocomposites with different f-MWNTs loadings at a cooling rate of 5 °C/min. In the case of neat PES, T_p is around 43.9 °C; however, T_ps shift to high temperature range in the presence of f-MWNTs. In the case of 99.5/0.5 and 99/1, T_ps shift to 48.8 and 53.1 °C, respectively. It is obvious that the variations in T_p are 4.9 °C and 4.3 °C with increasing f-MWNTs content from 0 to 0.5 wt% and 0.5 to 1 wt%, respectively; however, the increase in T_p is only 2.5 °C with further increasing f-MWNTs content from 1 to 2 wt%. It is also of interest to study the effect of cooling rates on the nonisothermal melt crystallization of neat PES and its nanocomposites. Fig. 2b

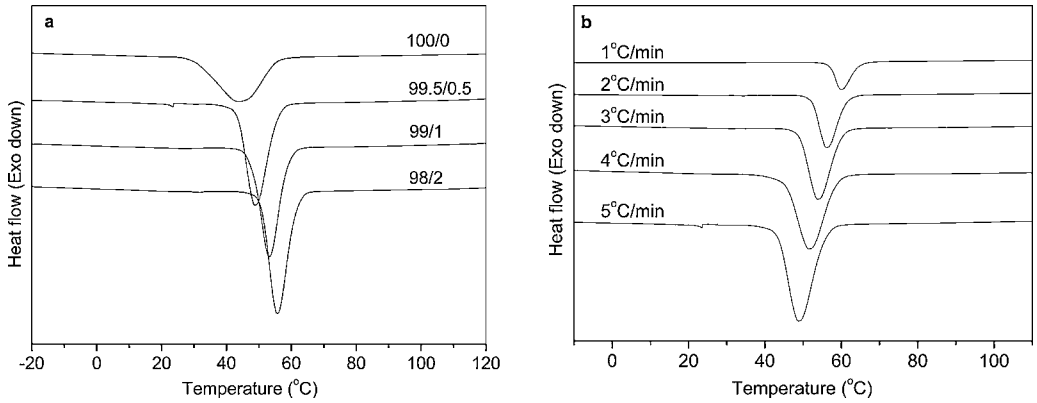

Fig. 2. (a) DSC traces of neat PES and its nanocomposites cooled from the melt at 5 °C/min and (b) DSC traces of 99/1 cooled from the melt at various cooling rates ranging from 1 to 5 °C/min.

shows the DSC traces of 99/1 at various cooling rates ranging from 1 to 5 °C/min as an example. It is clear from Fig. 2b that the crystallization exotherms shift to low temperature range with increasing the cooling rates from 1 to 5 °C/min since there is not enough time for the sample to crystallize at high temperature range at high cooling rates.

Fig. 3 summarizes the variation of T_ps with cooling rates for neat PES and its three nanocomposites with different f-MWNTs contents, from which the effects of cooling rates and f-MWNTs contents on the variation of T_ps of PES can be obtained clearly. It is obvious that T_p shifts to lower temperature range with increasing cooling rate for both neat PES and its nanocomposites. Meanwhile, T_ps of PES in the nanocomposites are higher than that of neat PES at a given cooling rate; moreover, T_ps shift to high temperature range with increasing the f-MWNTs contents in the nanocomposites. Such results indicate again that the nonisothermal melt crystallization of PES is enhanced by the presence of f-MWNTs, and the degree of enhancement in T_p is influenced by the f-MWNTs contents apparently. From the above studies, it is clear that the presence of f-MWNTs and their contents have a significant effect on the nonisothermal melt crystallization behavior of PES in the PES/f-MWNTs nanocomposites due to the heterogeneous nucleation agent effect of f-MWNTs. It should be noted that the ultimate degree of crystallinity values vary slightly around 35 ± 3% for both neat PES and its nanocomposites despite the cooling rates used in this study.

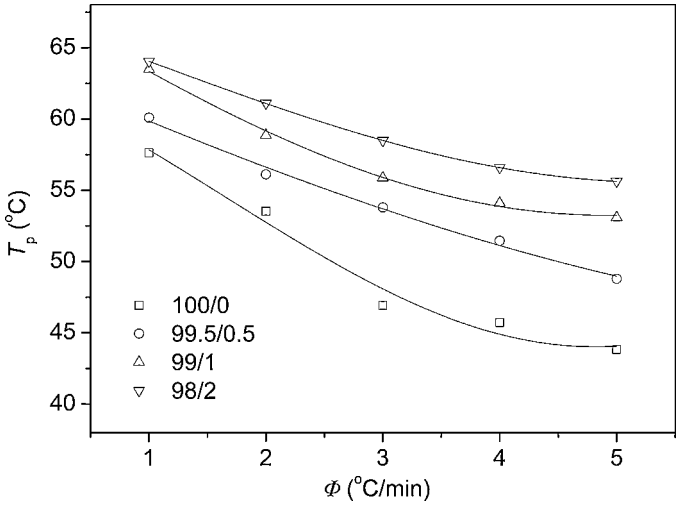

Fig. 3. Effect of cooling rates on the crystallization peak temperatures for neat PES and its nanocomposites.

The nonisothermal melt crystallization kinetics of neat PES and its nanocomposites was further studied. Parts a and b of Fig. 4 show the plots of relative degree of crystallinity ($X(T)$) versus crystallization temperature (T) for neat PES and 98/2, respectively. It is clear from Fig. 4 that the plots of $X(T)$ with T shift to low temperature range with increasing the cooling rate for both neat PES and 98/2. Moreover, the crystallization onset and end temperatures are higher in 98/2 than in neat PES at a given cooling rate, indicating again that the presence of f-MWNTs enhances the nonisothermal melt crystallization of PES in the PES/f-MWNTs nanocomposites. Several models [30–32] have been proposed for analyzing the nonisothermal melt crystallization kinetics of polymers. However, among these methods, the Ozawa method provides the parameters with more accurate physical meanings by assuming that the sample was cooled (or heated) with a constant rate from the molten state (or the amorphous state) [30]. The Ozawa equation can be expressed as

$$\log(-\ln(1 - X(T))) = \log K(T) - m \log \Phi \quad (1)$$

where $K(T)$ is the cooling function at a crystallization temperature T, $X(T)$ is the relative degree of crystallinity at a chosen temperature, Φ is the cooling rate, and m is the Ozawa exponent which depends on the type of nucleation and growth mechanism. However, it should be noted that the Ozawa method is not always applicable in polymer crystallization. Curvature is usually found in most cases in the respective plots when crystallization is studied at quite different cooling rates. The applicability of the Ozawa method may have to do with the narrow range of cooling rates; therefore, the cooling rates used in this study were from 1 to 5 °C/min. Fig. 5 shows the Ozawa plots for neat PES and 98/2, from which a series of parallel straight lines were obtained. It is obvious that the nonisothermal melt crystallization process of both neat PES and its nanocomposites can be described by the Ozawa method. The values of m and $K(T)$ were obtained and listed in Table 1 for comparison. The values of m are between 2.0 and 3.2 in the range of crystallization temperature from 44 to 65 °C, suggesting that the crystallization of PES suggests the three-dimensional truncated sphere growth with athermal nucleation [33]. Meanwhile, it can be seen that $K(T)$ decreases with increasing crystallization temperature, indicating that the crystallization is slowed down because of the difficulty in nucleation at high temperature.

3.3. *Effect of f-MWNTs on the isothermal melt crystallization of PES in the PES/f-MWNTs nanocomposites*

In the above section, the effect of f-MWNTs on the nonisothermal melt crystallization of PES in the PES/f-MWNTs was studied with DSC at various cooling rates. In this section, the effect of f-

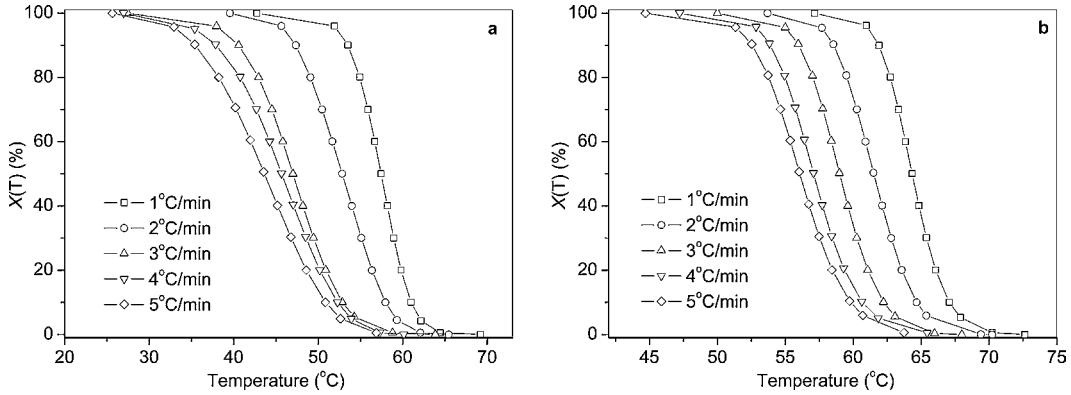

Fig. 4. Variation of $X(T)$ with T for (a) neat PES and (b) 98/2.

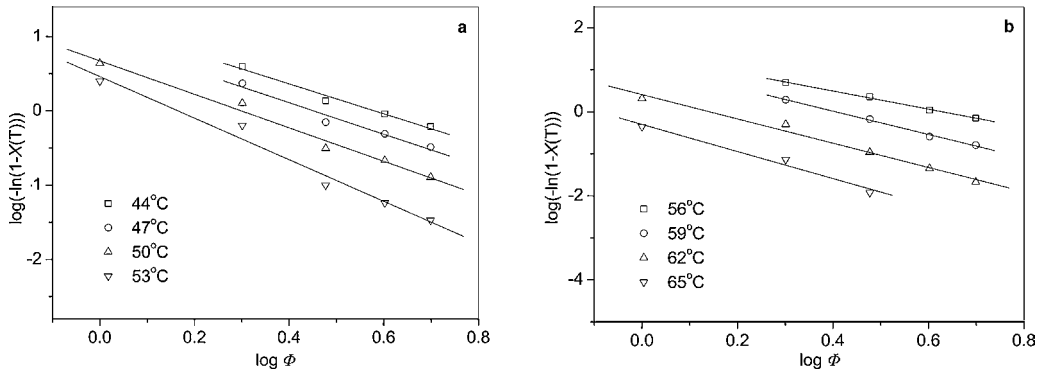

Fig. 5. The Ozawa plots of (a) neat PES and (b) 98/2.

MWNTs on the isothermal melt crystallization kinetics of PES in the PES/f-MWNTs was further investigated with DSC at different crystallization temperatures. Parts a and b of Fig. 6 show the development of relative degree of crystallinity (X_t) with crystallization time (t) for both neat PES and 99/1 at different T_cs, respectively. It is obvious that the crystallization time prolongs with increasing crystallization temperature for both neat PES and 99/1, suggesting that the crystallization is slowed down at high T_c. Moreover, at a given T_c of 64 °C, the crystallization finishes within around 10.4 min for neat PES, whereas the crystallization finished within around 2.41 min for 99/1. It is clear that the addition of f-MWNTs enhances the isothermal melt crystallization of PES significantly.

In order to analyze the isothermal melt crystallization kinetics of neat PES and its nanocomposites, the well-known Avrami method [34,35] is employed. It assumes that the relative degree of crystallinity X_t develops as a function of crystallization time t as follows:

$$1 - X_t = \exp(-kt^n) \tag{2}$$

where X_t is the relative crystallinity at time t, k is crystallization rate constant involving both nucleation and growth rate parameters, and n is Avrami exponent depending on the nature of nucleation and growth geometry of the crystals. For practical purpose, Eq. (2) is usually rearranged in its double logarithmic form as follows:

$$\log(-\ln(1 - Xt)) = \log k + n \log t \tag{3}$$

Parts a and b of Fig. 7 show the Avrami plots for both neat PES and 99/1, respectively, from which the values of n and k are

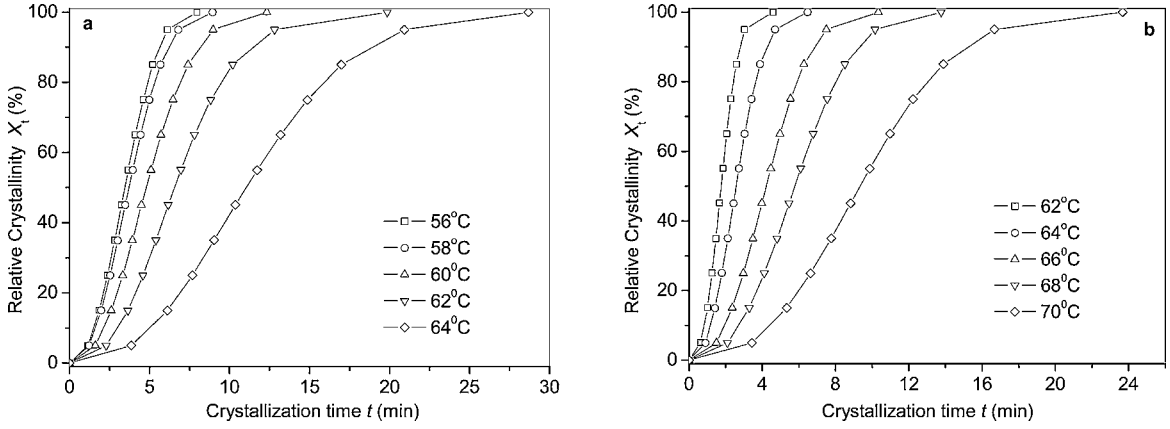

Fig. 6. Development of relative crystallinity (X_t) with crystallization time (t) for (a) neat PES and (b) 99/1.

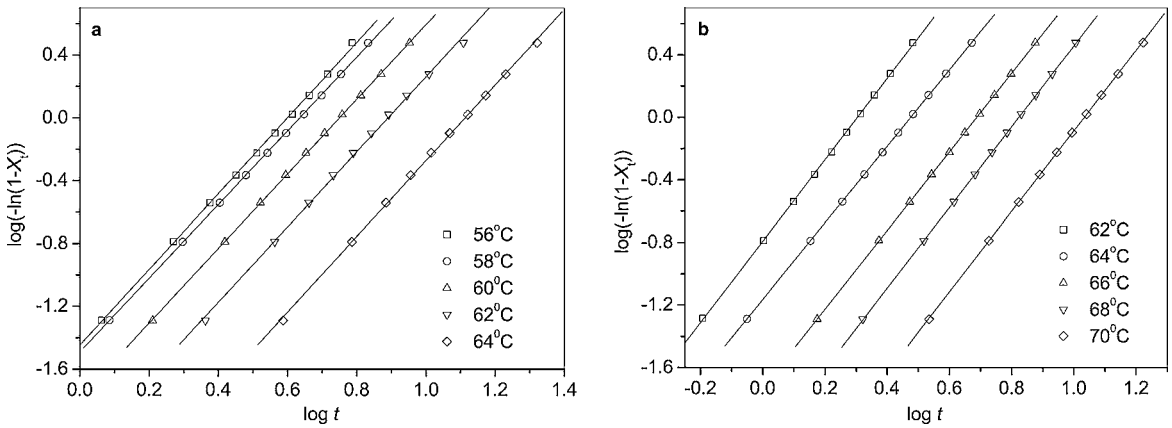

Fig. 7. The Avrami plots of (a) neat PES and (b) 99/1 at indicated crystallization temperatures.

obtained from the slopes and intercepts of the Avrami plots, respectively. All the related crystallization kinetics parameters for the overall isothermal melt crystallization of neat PES and its three nanocomposites with different f-MWNTs contents are listed in Table 2 for comparison. The average values of n for neat PES and its three nanocomposites are between 2.3 and 2.6 and are not affected significantly by the presence of f-MWNTs, indicating that the crystallization mechanism of PES does not change in the investigated T_cs. Moreover, the crystallization of PES suggests the three-dimensional truncated sphere growth with athermal nucleation [33].

However, it should be noted that it is difficult to compare the overall crystallization rate directly from the values of k because the unit of k is min^{-n} and n is not constant. Thus, the half-time of crystallization ($t_{0.5}$), the time required to achieve 50% of the final crystallinity of the samples, is an important parameter for the discussion of crystallization kinetics. Usually, the crystallization rate can also be easily described by the reciprocal of $t_{0.5}$. The value of $t_{0.5}$ is calculated by the following equation:

$$t_{0.5} = \left(\frac{\ln 2}{k}\right)^{1/n} \quad (4)$$

The values of $t_{0.5}$ and $1/t_{0.5}$ are listed in Table 2 for both neat PES and its three nanocomposites at different f-MWNTs contents. It can be seen that the values of $1/t_{0.5}$ decrease with increasing T_c for both neat PES and its nanocomposites, while the values of $t_{0.5}$ increase with increasing T_c. Such variations suggest that the overall isothermal crystallization rate decreases with increasing T_c for both neat PES and its nanocomposites. Moreover, the values of $t_{0.5}$ for the nanocomposites are smaller than those for neat PES at a given T_c such as 64 °C. Meanwhile, the values of $1/t_{0.5}$ increase with increasing the f-MWNTs content for the nanocomposites and are larger than those of neat PES, indicating again that the presence of f-MWNTs accelerates the crystallization process of PES in the nanocomposites.

Table 1
The Ozawa parameters for neat PES and its nanocomposites.

Samples	T_p (°C)	m	$K(T)$ (°C/min)^m
Neat PES	44	2.0	1.47×10^1
	47	2.1	9.00
	50	2.3	4.71
	53	2.8	2.90
PES/f-MWNTs 99.5/0.5	50	2.6	4.12×10^1
	53	3.2	3.12×10^1
	56	2.8	4.90
	59	3.1	1.48
PES/f-MWNTs 99/1	53	1.8	1.43×10^1
	56	2.6	1.25×10^1
	59	2.8	3.69
	62	3.2	1.13
PES/f-MWNTs 99/2	56	2.2	2.28×10^1
	59	2.8	1.33×10^1
	62	2.9	2.57
	65	3.2	5.01×10^{-1}

3.4. Effect of f-MWNTs on the spherulitic morphology and crystal structure of PES in the PES/f-MWNTs nanocomposites

In addition to the nonisothermal and isothermal melt crystallization of neat PES and its three nanocomposites, the effect of the presence of f-MWNTs on the spherulitic morphology of PES was studied with POM in this section. Fig. 8 illustrates the spherulitic morphology of neat PES and its nanocomposites crystallized at 60 °C. It can be seen from Fig. 8a that the well developed spherulites grow to a size of roughly several hundreds of microns in diameter in the case of neat PES. However, parts b, c and d of Fig. 8 show that the size of PES spherulites becomes smaller with increasing the f-MWNTs contents, suggesting a heterogeneous nucleation effect of f-MWNTs. On the basis of the POM study, it is clear that the nucle-

Table 2
The Avrami parameters for neat PES and its nanocomposites.

Samples	T_c (°C)	n	k (min^{-n})	$t_{0.5}$ (min)	$1/t_{0.5}$ (min^{-1})
Neat PES	56	2.4	3.58×10^{-2}	3.42	2.92×10^{-1}
	58	2.3	3.24×10^{-2}	3.69	2.71×10^{-1}
	60	2.4	1.66×10^{-2}	4.82	2.07×10^{-1}
	62	2.4	7.40×10^{-3}	6.67	1.50×10^{-1}
	64	2.4	2.07×10^{-3}	11.15	0.90×10^{-1}
PES/f-MWNTs 99.5/0.5	60	2.6	1.39×10^{-1}	1.87	5.35×10^{-1}
	62	2.5	5.33×10^{-2}	2.84	3.52×10^{-1}
	64	2.6	1.78×10^{-2}	4.13	2.42×10^{-1}
	66	2.6	6.99×10^{-3}	5.71	1.75×10^{-1}
	68	2.6	2.01×10^{-3}	9.60	1.04×10^{-1}
PES/f-MWNTs 99/1	62	2.6	1.61×10^{-1}	1.75	5.71×10^{-1}
	64	2.4	6.86×10^{-2}	2.57	3.89×10^{-1}
	66	2.5	1.86×10^{-2}	4.21	2.38×10^{-1}
	68	2.6	7.50×10^{-3}	5.77	1.73×10^{-1}
	70	2.6	2.19×10^{-3}	9.37	1.07×10^{-1}
PES/f-MWNTs 98/2	64	2.4	1.08×10^{-1}	2.18	4.59×10^{-1}
	66	2.5	3.69×10^{-2}	3.26	3.07×10^{-1}
	68	2.5	1.01×10^{-2}	5.46	1.83×10^{-1}
	70	2.6	3.46×10^{-3}	7.94	1.26×10^{-1}
	72	2.5	1.69×10^{-3}	11.42	0.88×10^{-1}

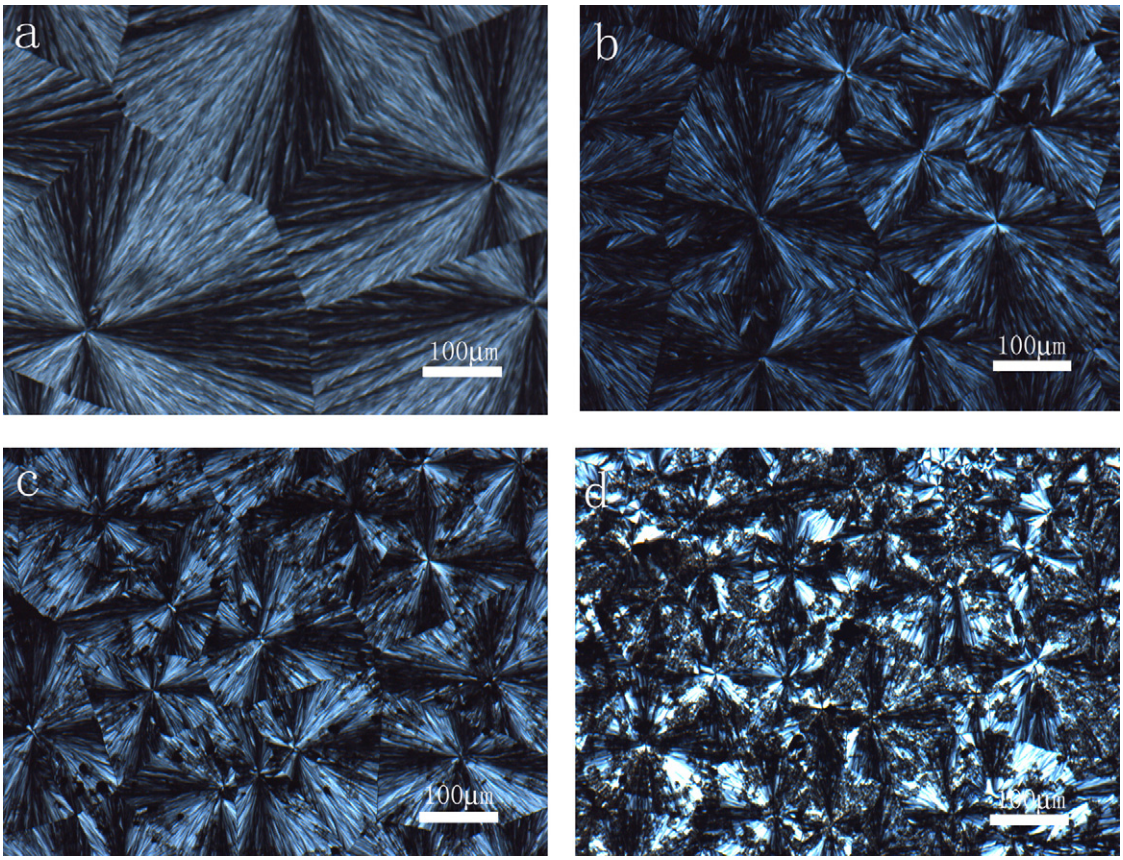

Fig. 8. Optical micrographs (same magnification, bar = 100 μm) of spherulitic morphology of neat PES and its nanocomposites after complete crystallization at 60 °C: (a) neat PES, (b) 99.5/0.5, (c) 99/1, and (d) 98/2.

ation density of PES spherulites is improved with increasing the f-MWNTs contents in the nanocomposites. Such results are consistent with the results in the previous section. In brief, the presence of f-MWNTs and their contents in the PES matrix have a significant influence on the spherulitic morphology and the overall crystallization process of PES in the nanocomposites.

It is also of importance and interest to study the presence of f-MWNTs on the crystal structure of PES in the PES/f-MWNTs nanocomposites. Fig. 9 illustrates the WAXD patterns of neat PES and its nanocomposites crystallized at 64 °C. Both neat PES and its nanocomposites exhibit almost the same diffraction peaks at

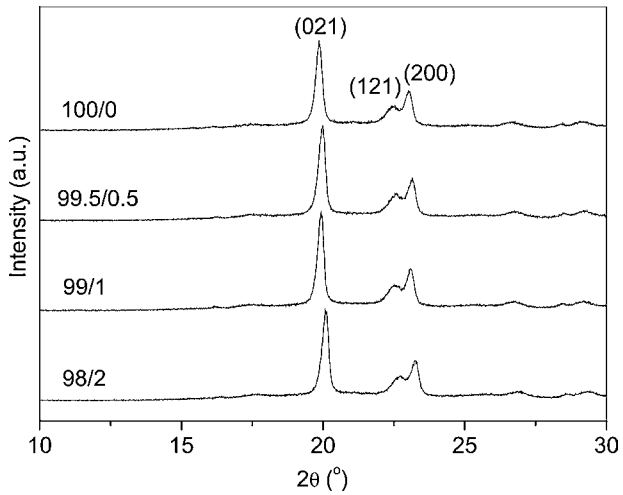

Fig. 9. WAXD patterns of neat PES and its nanocomposites.

almost the same locations. The three main diffraction peaks at around 19.9°, 22.5° and 23.0° are assigned to (0 2 1), (1 2 1) and (2 0 0) planes of α-form PES, respectively [1]. The degree of crystallinity values were calculated by the ratio of the area under the crystalline peaks to the whole area under both the crystalline peaks and the amorphous background on the basis of the WAXD patterns; thus, the degree of crystallinity values are estimated to be around 50 ± 2% for both neat PES and its three nanocomposites on the basis of the WAXD pattern in Fig. 9, indicating that the presence of f-MWNTs and the variation of the f-MWNTs contents from 0 to 2 wt% do not influence the degree of crystallinity of PES apparently in the PES/f-MWNTs nanocomposites. In brief, the incorporation of a small amount of f-MWNTs does not modify the crystal structure of PES and change the degree of crystallinity of PES in the PES/f-MWNTs nanocomposites significantly.

4. Conclusions

Biodegradable PES/f-MWNTs nanocomposites at different f-MWNTs loadings have been prepared successfully through solution casting method in this work. SEM observations indicate a homogeneous dispersion of f-MWNTs throughout the PES matrix. The effect of f-MWNTs on the nonisothermal melt crystallization, isothermal melt crystallization, spherulitic morphology, and crystal structure of PES in the nanocomposites was investigated with DSC, POM and WAXD in detail. The results show that both nonisothermal and isothermal melt crystallization of PES are enhanced by the presence of f-MWNTs and influenced by the f-MWNTs contents due to the nucleation effect induced by f-MWNTs. The nonisothermal melt crystallization kinetics of neat PES and its nanocomposites was successfully described by the Ozawa method, while the isothermal

melt crystallization kinetics of neat PES and its nanocomposites was successfully described by the Avrami method. The values of the exponents in the Ozawa and Avrami fits suggest three-dimensional truncated sphere growth with athermal nucleation for both neat PES and the PES/f-MWNTs nanocomposites. In the case of isothermal crystallization kinetics, the crystallization rate of PES is enhanced significantly while the crystallization mechanism does not change in the presence of f-MWNTs in the nanocomposites. The crystal structure of PES does not change in the PES/f-MWNTs nanocomposites despite the presence of f-MWNTs.

Acknowledgements

Part of this work is financially supported by the Graduate Innovative Foundation of Beijing University of Chemical Technology (09Ma011) and National Natural Science Foundation, China (Grant No. 20974012).

References

[1] A.S. Ueda, Y. Chatani, H. Tadokoro, Polym. J. 2 (1971) 387–391.
[2] Z.H. Gan, H. Abe, Y. Doi, Biomacromolecules 1 (2000) 704–712.
[3] Z.H. Gan, H. Abe, Y. Doi, Biomacromolecules 1 (2000) 713–720.
[4] T. Iwata, Y. Doi, K. Isono, Y. Yoshida, Macromolecules 34 (2001) 7343–7348.
[5] Z.B. Qiu, T. Ikehara, T. Nishi, Polymer 44 (2003) 5429–5437.
[6] Z.B. Qiu, M. Komura, T. Ikehara, T. Nishi, Polymer 44 (2003) 7781–7785.
[7] G.Z. Papageorgiou, D.N. Bikiaris, D.S. Achilias, Thermochim. Acta 457 (2007) 41–54.
[8] Z.B. Qiu, T. Ikehara, T. Nishi, Macromolecules 35 (2002) 8251–8254.
[9] J.M. Lu, Z.B. Qiu, W.T. Yang, Macromolecules 41 (2008) 141–148.
[10] Z.B. Qiu, S. Fujinami, M. Komura, K. Nakajima, T. Ikehara, T. Nishi, Polymer 45 (2004) 4355–4360.
[11] H.L. Chen, S.F. Wang, Polymer 41 (2000) 5157–5164.
[12] H.A. Al-Salah, Polym. Bull. 41 (1998) 593–600.
[13] T. Ikehara, H. Kimura, T. Kataoka, J. Polym. Sci. B: Polym. Phys. 48 (2010) 706–711.
[14] L.Q. Miao, Z.B. Qiu, W.T. Yang, T. Ikehara, React. Funct. Polym. 68 (2008) 446–457.
[15] S. Iijima, Nature 354 (1991) 56–58.
[16] M. Moniruzzaman, K.I. Winey, Macromolecules 39 (2006) 5194–5205.
[17] S. Huang, M. Wang, T.X. Liu, W.D. Zhang, W.C. Tjiu, C.B. He, X.H. Lu, Polym. Eng. Sci. 49 (2009) 1063–1068.
[18] T.X. Liu, I.Y. Phang, L. Shen, S.Y. Chow, W.D. Zhang, Macromolecules 37 (2004) 7214–7222.
[19] S.F. Wang, L. Shen, W.D. Zhang, Y.J. Tong, Biomacromolecules 6 (2005) 3067–3072.
[20] J.F. Gao, D.X. Yan, H.D. Huang, K. Dai, Z.M. Li, J. Appl. Polym. Sci. 114 (2009) 1002–1010.
[21] J.Z. Xu, T. Chen, C.L. Yang, Z.M. Li, Y.M. Mao, B.Q. Zeng, B.S. Hsiao, Macromolecules 43 (2010) 5000–5008.
[22] X. Hu, H.N. An, Z.M. Li, Y. Geng, L.B. Li, C.L. Yang, Macromolecules 42 (2009) 3215–3218.
[23] H.S. Xu, X.J. Dai, P.R. Lamb, Z.M. Li, J. Polym. Sci. B: Polym. Phys. 47 (2009) 2341–2352.
[24] J. Ramontja, S.S. Ray, S.K. Pillai, A.S. Luyt, Macromol. Mater. Eng. 294 (2009) 839–846.
[25] Y.Y. Zhao, Z.B. Qiu, W.T. Yang, J. Phys. Chem. B 112 (2008) 16461–16468.
[26] Z.B. Qiu, S.Y. Zhu, W.T. Yang, J. Nanosci. Nanotechnol. 9 (2009) 4961–4969.
[27] L. Song, Z.B. Qiu, Polym. Degrad. Stab. 94 (2009) 632–637.
[28] Y.Y. Zhao, Z.B. Qiu, W.T. Yang, Compos. Sci. Technol. 69 (2009) 627–632.
[29] C.L. Xu, Z.B. Qiu, J. Polym. Sci. B: Polym. Phys. 47 (2009) 2238–2246.
[30] T. Ozawa, Polymer 12 (1971) 150–158.
[31] A. Jeziorny, Polymer 19 (1978) 1142–1144.
[32] A.K. Gupta, S.T. Purwar, J. Appl. Polym. Sci. 29 (1984) 1595–1609.
[33] B. Wunderlich, Macromolecular Physics, vol. 2, Academic Press, New York, 1976.
[34] M. Avrami, J. Chem. Phys. 8 (1939) 212–224.
[35] M. Avrami, J. Chem. Phys. 9 (1941) 177–184.